

# Nodal superconductivity in $\text{Ba}(\text{Fe}_{1-x}\text{Ru}_x)_2\text{As}_2$ induced by isovalent Ru substitution

X. Qiu,<sup>1</sup> S. Y. Zhou,<sup>1</sup> H. Zhang,<sup>1</sup> B. Y. Pan,<sup>1</sup> X. C. Hong,<sup>1</sup> Y. F. Dai,<sup>1</sup> Man Jin Eom,<sup>2</sup> Jun Sung Kim,<sup>2</sup> S. Y. Li<sup>1,\*</sup>

<sup>1</sup>*Department of Physics, State Key Laboratory of Surface Physics,*

*and Laboratory of Advanced Materials, Fudan University, Shanghai 200433, China*

<sup>2</sup>*Department of Physics, Pohang University of Science and Technology, Pohang 790-784, Korea*

(Dated: August 18, 2024)

We present the ultra-low-temperature heat transport study of an iron-based superconductor  $\text{Ba}(\text{Fe}_{0.64}\text{Ru}_{0.36})_2\text{As}_2$  ( $T_c = 20.2$  K), in which the superconductivity is induced by isovalent Ru substitution. In zero field we find a large residual linear term  $\kappa_0/T$ , more than 40% of the normal-state value. At low field, the  $\kappa_0/T$  shows an  $H^{1/2}$  dependence. These provide strong evidences for nodes in the superconducting gap of  $\text{Ba}(\text{Fe}_{0.64}\text{Ru}_{0.36})_2\text{As}_2$ , which mimics that in another isovalently substituted superconductor  $\text{BaFe}_2(\text{As}_{1-x}\text{P}_x)_2$ . Our results show that the isovalent Ru substitution can also induce nodal superconductivity in  $\text{BaFe}_2\text{As}_2$ , as P does, and they may have the same origin. We further compare them with other two nodal superconductors  $\text{LaFePO}$  and  $\text{LiFeP}$ .

PACS numbers: 74.70.Xa, 74.25.fc, 74.20.Rp

Since the discovery of high- $T_c$  superconductivity in iron-based compounds [1, 2], the electronic pairing mechanism has been a central issue [3]. One key to understand it is to clarify the symmetry and structure of the superconducting gap [4]. However, even for the most studied (Ba,Sr,Ca,Eu) $\text{Fe}_2\text{As}_2$  (122) system, the situation is still fairly complex [4].

Near optimal doping, for both hole- and electron-doped 122 compounds, the angle-resolved photon emission spectroscopy (ARPES) experiments clearly demonstrated multiple nodeless superconducting gaps [5, 6], which was further supported by bulk measurements such as thermal conductivity [7–9]. On the overdoped side, nodal superconductivity was found in the extremely hole-doped  $\text{KFe}_2\text{As}_2$  [10, 11], while strongly anisotropic gap [9], or isotropic gaps with significantly different magnitude [12, 13] were suggested in the heavily electron-doped  $\text{Ba}(\text{Fe}_{1-x}\text{Co}_x)_2\text{As}_2$ . On the underdoped side, recent heat transport measurements claimed possible nodes in the superconducting gap of hole-doped  $\text{Ba}_{1-x}\text{K}_x\text{Fe}_2\text{As}_2$  with  $x < 0.16$  [14], in contrast to the nodeless gaps found in electron-doped  $\text{Ba}(\text{Fe}_{1-x}\text{Co}_x)_2\text{As}_2$  [9].

Intriguingly, nodal superconductivity was also found in  $\text{BaFe}_2(\text{As}_{1-x}\text{P}_x)_2$  ( $T_c = 30$  K) [15, 16], in which the superconductivity is induced by the isovalent P substitution for As. The laser-ARPES experiments on  $\text{BaFe}_2(\text{As}_{0.65}\text{P}_{0.35})_2$  showed isotropic gaps in the three hole pockets around the Brillouin zone (BZ) center, therefore the gap nodes must locate on the electron pockets around the BZ corners [17]. Moreover, previously  $\text{LaFePO}$  ( $T_c \sim 6$  K) displays clear nodal behavior [18–20], and recently there is penetration depth evidence for nodes in the superconducting gap of  $\text{LiFeP}$  ( $T_c \sim 4.5$  K) [21]. The nodal superconductivity in these P-substituted compounds are very striking, which raises the puzzling question why the P substitution is so special in iron-based superconductors. The theoretical explanations of this puzzle are far from consensus [22–25].

In the  $\text{Fe}_2\text{As}_2$  slabs of iron arsenides shown in Fig. 1, instead of substituting As with P, there is an alternative way for isovalent substitution, to substitute Fe with Ru. Indeed, superconductivity with  $T_c$  up to 20 K was found in  $\text{Ba}(\text{Fe}_{1-x}\text{Ru}_x)_2\text{As}_2$  [26] and  $\text{Sr}(\text{Fe}_{1-x}\text{Ru}_x)_2\text{As}_2$  [27]. The phase diagram of  $\text{Ba}(\text{Fe}_{1-x}\text{Ru}_x)_2\text{As}_2$  is very similar to that of  $\text{BaFe}_2(\text{As}_{1-x}\text{P}_x)_2$  [28, 29]. The ARPES measurements on  $\text{Ba}(\text{Fe}_{0.65}\text{Ru}_{0.35})_2\text{As}_2$  showed that Ru induces neither hole nor electron doping, but the hole and electron pockets are about twice larger than in  $\text{BaFe}_2\text{As}_2$  [30]. To investigate the superconducting gap structure in these Ru-substituted superconductors may help to solve above puzzle of P substitution.

In this Letter, we report the demonstration of nodal superconductivity in optimally substituted  $\text{Ba}(\text{Fe}_{0.64}\text{Ru}_{0.36})_2\text{As}_2$  by thermal conductivity measurements down to 50 mK. Our finding shows that the nodal superconducting states in P-substituted iron arsenides are not that special, and suggests a common origin of the nodal superconductivity induced by isovalent substitutions, at least in  $\text{Ba}(\text{Fe}_{1-x}\text{Ru}_x)_2\text{As}_2$  and  $\text{BaFe}_2(\text{As}_{1-x}\text{P}_x)_2$ .

Single crystals of optimally substituted  $\text{Ba}(\text{Fe}_{0.64}\text{Ru}_{0.36})_2\text{As}_2$  were grown using a self-flux method [31]. Plate-shaped crystals with shiny surfaces were extracted mechanically. The Ru substituting level was determined by energy dispersive X-ray spectroscopy. The dc magnetic susceptibility was measured at  $H = 10$  Oe, with zero-field cooled, using a SQUID (MPMS, Quantum Design). The sample was cleaved to a rectangular shape of dimensions  $1.50 \times 0.68$  mm<sup>2</sup> in the  $ab$ -plane, with 70  $\mu\text{m}$  thickness along the  $c$ -axis. Contacts were made directly on the sample surfaces with silver paint, which were used for both resistivity and thermal conductivity measurements. The contacts are metallic with typical resistance 200 m $\Omega$  at 1.5 K. In-plane thermal conductivity was measured in a dilution refrigerator, using a standard four-wire

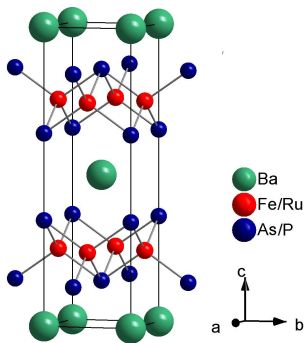


FIG. 1: (Color online). Crystal structure of  $\text{BaFe}_2\text{As}_2$ . There are two ways for isovalent substitution in the  $\text{Fe}_2\text{As}_2$  slabs, substituting As with P, or Fe with Ru. Both substitutions can induce superconductivity, and result in similar phase diagrams.

steady-state method with two  $\text{RuO}_2$  chip thermometers, calibrated *in situ* against a reference  $\text{RuO}_2$  thermometer. Magnetic fields were applied along the  $c$ -axis. To ensure a homogeneous field distribution in the sample, all fields were applied at temperature above  $T_c$ .

Fig. 2a shows the in-plane resistivity  $\rho(T)$  of our  $\text{Ba}(\text{Fe}_{0.64}\text{Ru}_{0.36})_2\text{As}_2$  single crystal. The magnitude and shape of  $\rho(T)$  are consistent with previous report [28]. The normalized magnetization was plotted in the inset, which displays a nice superconducting transition at about 20 K. According to the phase diagram of  $\text{Ba}(\text{Fe}_{1-x}\text{Ru}_x)_2\text{As}_2$  [28, 29], no static magnetic order exists in our optimally substituted sample. The resistivity data between 30 and 90 K are fitted to  $\rho(T) = \rho_0 + AT^n$ , which gives a residual resistivity  $\rho_0 = 43.7 \pm 0.1 \mu\Omega\text{cm}$  and  $n = 1.31 \pm 0.1$ . Such a non-Fermi-liquid temperature dependence of  $\rho(T)$  is similar to that observed in  $\text{BaFe}_2(\text{As}_{1-x}\text{P}_x)_2$  near optimal substitution, which may reflect the presence of antiferromagnetic spin fluctuations near a quantum critical point [32].

The low-temperature part of  $\rho(T)$  is plotted in Fig. 2b. The zero-resistance point of the resistive transition is at  $T_c = 20.2$  K, which is in good agreement with the diamagnetic superconducting transition shown in the inset of Fig. 2a. To estimate the upper critical field  $H_{c2}$ , the resistivity in  $H = 3, 6, 9,$  and  $14.5$  T with  $H||c$  were also measured, as seen in Fig. 2b. Fig. 2c shows the temperature dependence of  $H_{c2}$ , defined by  $\rho = 0$  and  $\rho = 0.1\rho_N$ , respectively. For comparison, the  $H_{c2}(T)$  of the electron-doped  $\text{Ba}(\text{Fe}_{0.9}\text{Co}_{0.1})_2\text{As}_2$  single crystal with  $T_c \approx 22$  K is reproduced from ref. [33]. One can see that although the  $T_c$  of our  $\text{Ba}(\text{Fe}_{0.64}\text{Ru}_{0.36})_2\text{As}_2$  is only slightly lower than  $\text{Ba}(\text{Fe}_{0.9}\text{Co}_{0.1})_2\text{As}_2$ , its  $H_{c2}(T)$  is significantly lower. For  $\text{Ba}(\text{Fe}_{0.9}\text{Co}_{0.1})_2\text{As}_2$ , extrapolation of the  $H_{c2}(T)$  data suggests  $H_{c2}(0)$  between 40 and 50 T, much larger than that obtained from Werthamer-Helfand-Hohenberg formula  $H_{c2}^{WHH}(0) = -0.69T_c dH_{c2}/dT|_{T=T_c}$  [33]. For our

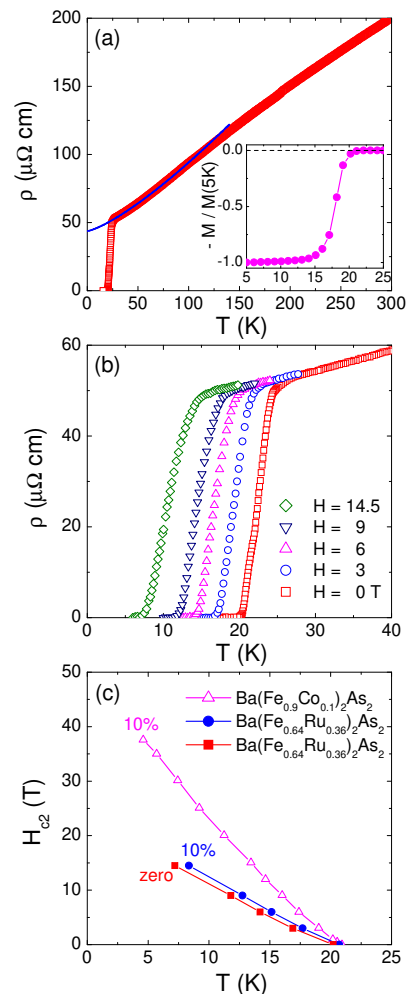


FIG. 2: (Color online). (a) In-plane resistivity of  $\text{Ba}(\text{Fe}_{0.64}\text{Ru}_{0.36})_2\text{As}_2$  single crystal. The solid line is a fit of the data between 30 and 90 K to  $\rho(T) = \rho_0 + AT^n$ . Inset: normalized magnetization. (b) Low-temperature resistivity in  $H = 0, 3, 6, 9,$  and  $14.5$  T with  $H||c$ . (c) Temperature dependence of the upper critical field  $H_{c2}$ . The squares and circles represent  $H_{c2}$  of  $\text{Ba}(\text{Fe}_{0.64}\text{Ru}_{0.36})_2\text{As}_2$  defined by  $\rho = 0$  and  $\rho = 0.1\rho_N$ , respectively. The triangles represent  $H_{c2}$  of  $\text{Ba}(\text{Fe}_{0.9}\text{Co}_{0.1})_2\text{As}_2$  with  $T_c \approx 22$  K [33].

$\text{Ba}(\text{Fe}_{0.64}\text{Ru}_{0.36})_2\text{As}_2$ ,  $H_{c2}^{WHH}(0) \approx 15.3$  T is obtained, which is also apparently lower than the actual  $H_{c2}(0)$ . We can only roughly estimate the bulk  $H_{c2}(0) \approx 23$  T, defined by  $\rho = 0$ , by linearly extrapolating the data between 6 and 14.5 T in Fig. 2c. Note that a slightly different  $H_{c2}(0)$  does not affect our discussion below.

Fig. 3 shows the temperature dependence of the in-plane thermal conductivity for  $\text{Ba}(\text{Fe}_{0.64}\text{Ru}_{0.36})_2\text{As}_2$  in  $H = 0, 1, 2, 4, 6, 9,$  and  $12$  T magnetic fields, plotted as  $\kappa/T$  vs  $T$ . All the curves are roughly linear, as previously observed in  $\text{BaFe}_{1.9}\text{Ni}_{0.1}\text{As}_2$  [8],  $\text{KFe}_2\text{As}_2$  [10], and overdoped  $\text{Ba}(\text{Fe}_{1-x}\text{Co}_x)_2\text{As}_2$  single crystals [9, 12]. Therefore we fit all the curves to  $\kappa/T = a + bT^{\alpha-1}$  with  $\alpha$  fixed to 2. The two terms  $aT$  and  $bT^\alpha$  represent contri-

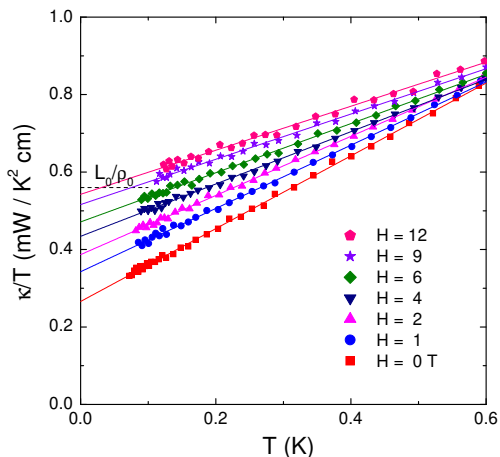


FIG. 3: (Color online). Low-temperature in-plane thermal conductivity of  $\text{Ba}(\text{Fe}_{0.64}\text{Ru}_{0.36})_2\text{As}_2$  in magnetic fields applied along the  $c$ -axis ( $H = 0, 1, 2, 4, 6, 9$  and  $12$  T). The solid lines are  $\kappa/T = a + bT$  fit to all the curves, respectively. The dash line is the normal-state Wiedemann-Franz law expectation  $L_0/\rho_0$ , with  $L_0$  the Lorenz number  $2.45 \times 10^{-8} \text{ W}\Omega\text{K}^{-2}$  and  $\rho_0 = 43.7 \mu\Omega\text{cm}$ .

contributions from electrons and phonons, respectively. Here we only focus on the electronic term.

In zero field, the fitting gives a residual linear term  $\kappa_0/T = 0.266 \pm 0.002 \text{ mW K}^{-2} \text{ cm}^{-1}$ . This value is more than 40% of the normal-state Wiedemann-Franz law expectation  $\kappa_{N0}/T = L_0/\rho_0 = 0.56 \text{ mW K}^{-2} \text{ cm}^{-1}$ , with  $L_0$  the Lorenz number  $2.45 \times 10^{-8} \text{ W}\Omega\text{K}^{-2}$  and  $\rho_0 = 43.7 \mu\Omega\text{cm}$ . For another isovalently substituted  $\text{BaFe}_2(\text{As}_{0.67}\text{P}_{0.33})_2$  single crystal, similar value of  $\kappa_0/T \approx 0.25 \text{ mW K}^{-2} \text{ cm}^{-1}$  was obtained, which is about 30% of its normal-state  $\kappa_{N0}/T$  [16]. The significant  $\kappa_0/T$  of  $\text{Ba}(\text{Fe}_{0.64}\text{Ru}_{0.36})_2\text{As}_2$  in zero field is a strong evidence for nodes in the superconducting gap [34].

The field dependence of  $\kappa_0/T$  may provide further support for the nodes [34]. In Fig. 4, the normalized  $(\kappa_0/T)/(\kappa_{N0}/T)$  of  $\text{Ba}(\text{Fe}_{0.64}\text{Ru}_{0.36})_2\text{As}_2$  is plotted as a function of  $H/H_{c2}$ , with the normal-state  $\kappa_{N0}/T = 0.56 \text{ mW K}^{-2} \text{ cm}^{-1}$  and bulk  $H_{c2} = 23$  T. Similar data of the clean  $s$ -wave superconductor Nb [35], an overdoped  $d$ -wave cuprate superconductor Tl-2201 [36], and  $\text{BaFe}_2(\text{As}_{0.67}\text{P}_{0.33})_2$  [16] are also plotted for comparison. For a nodal superconductor in magnetic field, delocalized states exist out the vortex cores and dominate the heat transport in the vortex state, in contrast to the  $s$ -wave superconductor. At low field, the Doppler shift due to superfluid flow around the vortices will yield an  $H^{1/2}$  growth in quasiparticle density of states (the Volovik effect [37]), thus the  $H^{1/2}$  field dependence of  $\kappa_0/T$ . From Fig. 4, the behavior of  $\kappa_0(H)/T$  in  $\text{Ba}(\text{Fe}_{0.64}\text{Ru}_{0.36})_2\text{As}_2$  clearly mimics that in Tl-2201 and  $\text{BaFe}_2(\text{As}_{0.67}\text{P}_{0.33})_2$ . In the inset of Fig. 4, the  $\kappa_0(H)/T$  of  $\text{Ba}(\text{Fe}_{0.64}\text{Ru}_{0.36})_2\text{As}_2$  obeys the  $H^{1/2}$  dependence at low field, which supports the existence of nodes in the

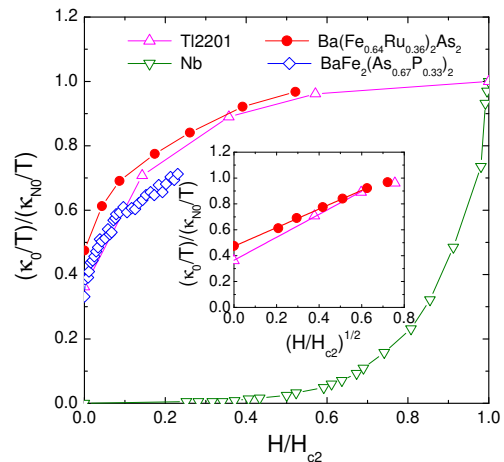


FIG. 4: (Color online). Normalized residual linear term  $\kappa_0/T$  of  $\text{Ba}(\text{Fe}_{0.64}\text{Ru}_{0.36})_2\text{As}_2$  as a function of  $H/H_{c2}$ . Similar data of the clean  $s$ -wave superconductor Nb [35], an overdoped  $d$ -wave cuprate superconductor Tl-2201 [36], and  $\text{BaFe}_2(\text{As}_{0.67}\text{P}_{0.33})_2$  [16] are also shown for comparison. The behavior of  $\kappa_0(H)/T$  in  $\text{Ba}(\text{Fe}_{0.64}\text{Ru}_{0.36})_2\text{As}_2$  clearly mimics that in Tl-2201 and  $\text{BaFe}_2(\text{As}_{0.67}\text{P}_{0.33})_2$ . Inset: the same data of  $\text{Ba}(\text{Fe}_{0.64}\text{Ru}_{0.36})_2\text{As}_2$  and Tl-2201 plotted against  $(H/H_{c2})^{1/2}$ . The lines represent the  $H^{1/2}$  dependence.

superconducting gap.

To our knowledge, previously there are five iron-based superconductors displaying nodal superconductivity,  $\text{KFe}_2\text{As}_2$  [10, 11], underdoped  $\text{Ba}_{1-x}\text{K}_x\text{Fe}_2\text{As}_2$  ( $x < 0.16$ ) [14],  $\text{BaFe}_2(\text{As}_{1-x}\text{P}_x)_2$  [15, 16],  $\text{LaFePO}$  [18–20], and  $\text{LiFeP}$  [21]. Here we only consider the “in-plane nodes”, not counting the “ $c$ -axis nodes” in underdoped and overdoped  $\text{Ba}(\text{Fe}_{1-x}\text{Co}_x)_2\text{As}_2$  as suggested by  $c$ -axis heat transport experiments [38]. For the extremely hole-doped  $\text{KFe}_2\text{As}_2$ , the nodal superconductivity may result from the intraband pairing via antiferromagnetic fluctuations, due to the lack of electron pockets [10]. For underdoped  $\text{Ba}_{1-x}\text{K}_x\text{Fe}_2\text{As}_2$ , it is still not clear how the superconducting gap transforms from nodeless to nodal at  $x \approx 0.16$  [14]. The rest three compounds,  $\text{BaFe}_2(\text{As}_{1-x}\text{P}_x)_2$ ,  $\text{LaFePO}$ , and  $\text{LiFeP}$ , have stimulated various interpretations of the effect of isovalent P substitution on the superconducting gap structure [22–25].

Our new finding of nodal superconductivity in  $\text{Ba}(\text{Fe}_{0.64}\text{Ru}_{0.36})_2\text{As}_2$  reveals the similarity between the isovalently Ru- and P-substituted iron arsenides, therefore the P substitution is not that special for inducing nodal superconductivity. In this sense, the mystery of P substitution in iron-based superconductors has been partially unwrapped. What next one needs to do is to find out whether there is a common origin for the nodal superconductivity in these isovalently substituted compounds.

Due to the smaller size of P ion than As ion, one common structural feature of the P-substituted compounds is the decrease of pnictogen height and increase of As-Fe-

As angle [32, 40, 41]. The substitution of larger Ru ion for Fe ion in  $\text{Ba}(\text{Fe}_{1-x}\text{Ru}_x)_2\text{As}_2$  results in the increase of  $a$  lattice parameter and decrease of  $c$  lattice parameter, thus the decrease of pnictogen height and increase of As-Fe-As angle too [28]. Therefore, both the P and Ru substitutions cause the same trend of structure change in iron arsenides.

LaFePO and LiFeP belong to the “1111” and “111” systems, respectively, and the P ions have fully substituted As ions in LaFeAsO and LiFeAs. This is different from the partial P and Ru substitution in superconducting  $\text{BaFe}_2(\text{As}_{1-x}\text{P}_x)_2$  and  $\text{Ba}(\text{Fe}_{1-x}\text{Ru}_x)_2\text{As}_2$ . In fact, both the fully substituted  $\text{BaFe}_2\text{P}_2$  and  $\text{BaRu}_2\text{As}_2$  are nonsuperconducting [42, 43]. Another difference is the much lower  $T_c$  of LaFePO and LiFeP, 6 and 4.5 K, respectively. For LaFePO, Kuroki *et al.* have attributed the low- $T_c$  nodal pairing to the lack of Fermi surface  $\gamma$  around  $(\pi, \pi)$  in the unfolded Brillouin zone, due to the low pnictogen height [22]. Hashimoto *et al.* also related the nodal superconductivity in LiFeP to the pnictogen height [21].

For  $\text{Ba}(\text{Fe}_{1-x}\text{Ru}_x)_2\text{As}_2$  and  $\text{BaFe}_2(\text{As}_{1-x}\text{P}_x)_2$ , the substitutions start from the same parent compound  $\text{BaFe}_2\text{As}_2$ , and result in similar phase diagrams [28, 29]. The highest  $T_c$  at optimal substitution, 20 and 30 K, are also close. Furthermore, the Fermi surface structures are roughly similar, with hole pockets around BZ center and electron pockets around BZ corners [17, 30]. All these similarities suggest that the origin of the nodal superconductivity in  $\text{Ba}(\text{Fe}_{1-x}\text{Ru}_x)_2\text{As}_2$  and  $\text{BaFe}_2(\text{As}_{1-x}\text{P}_x)_2$  may be the same. Suzuki *et al.* have proposed three-dimensional nodal structure in the largely warped hole Fermi surface and no nodes on the electron Fermi surface [25]. However, these seem inconsistent with the ARPES results, which have constrained the nodes on the electron pockets [17]. More careful considerations of the structural parameters, band structure, and local interactions are needed to clarify whether there is a common origin for the nodal superconductivity in all these isovalently substituted iron arsenides.

In summary, we have measured the thermal conductivity of  $\text{Ba}(\text{Fe}_{0.64}\text{Ru}_{0.36})_2\text{As}_2$  single crystal down to 50 mK. A large  $\kappa_0/T$  at zero field and an  $H^{1/2}$  field dependence of  $\kappa_0(H)/T$  at low field give strong evidences for nodal superconductivity in  $\text{Ba}(\text{Fe}_{0.64}\text{Ru}_{0.36})_2\text{As}_2$ . Comparing with previous P-substituted iron arsenides, our new finding suggest that the nodal superconductivity induced by isovalent substitutions may have the same origin, at least in  $\text{Ba}(\text{Fe}_{1-x}\text{Ru}_x)_2\text{As}_2$  and  $\text{BaFe}_2(\text{As}_{1-x}\text{P}_x)_2$ . Finding out this origin will be important for getting a complete electronic pairing mechanism of the iron-based high- $T_c$  superconductors.

This work is supported by the Natural Science Foundation of China, the Ministry of Science and Technology of China (National Basic Research Program No: 2009CB929203), Program for New Century

Excellent Talents in University, Program for Professor of Special Appointment (Eastern Scholar) at Shanghai Institutions of Higher Learning, and STCSM of China (No: 08dj1400200 and 08PJ1402100).

\* E-mail: shiyan\_li@fudan.edu.cn

- 
- [1] Y. Kamihara *et al.*, J. Am. Chem. Soc. **130**, 3296 (2008).
  - [2] J. Paglione and R. L. Greene, Nature Physics **6**, 645 (2010).
  - [3] Fa Wang and Dung-hai Lee, Science **332**, 200 (2011).
  - [4] P. J. Hirschfeld, M. M. Korshunov, and I. I. Mazin, arXiv:1106.3712, and references therein.
  - [5] H. Ding *et al.*, EPL **83**, 47001 (2008).
  - [6] K. Terashima *et al.*, Proc. Natl. Acad. Sci. **106**, 7330 (2009).
  - [7] X. G. Luo *et al.*, Phys. Rev. B **80**, 140503(R) (2009).
  - [8] L. Ding *et al.*, New J. Phys. **11**, 093018 (2009).
  - [9] M. A. Tanatar *et al.*, Phys. Rev. Lett. **104**, 067002 (2010).
  - [10] J. K. Dong *et al.*, Phys. Rev. Lett. **104**, 087005 (2010).
  - [11] K. Hashimoto *et al.*, Phys. Rev. B **82**, 014526 (2010).
  - [12] J. K. Dong *et al.*, Phys. Rev. B **81**, 094520 (2010).
  - [13] Yunkyu Bang, Phys. Rev. Lett. **104**, 217001 (2010).
  - [14] J.-Ph. Reid *et al.*, arXiv:1105.2232.
  - [15] Y. Nakai *et al.*, Phys. Rev. B **81**, 020503(R) (2010).
  - [16] K. Hashimoto *et al.*, Phys. Rev. B **81**, 220501(R) (2010).
  - [17] T. Shimojima *et al.*, Science **332**, 564 (2011).
  - [18] J. D. Fletcher *et al.*, Phys. Rev. Lett. **102**, 147001 (2009).
  - [19] C. W. Hicks *et al.*, Phys. Rev. Lett. **103**, 127003 (2009).
  - [20] M. Yamashida *et al.*, Phys. Rev. B **80**, 220509 (2009).
  - [21] K. Hashimoto *et al.*, to be published.
  - [22] K. Kuroki *et al.*, Phys. Rev. B **79**, 224511 (2009).
  - [23] F. Wang, H. Zhai, and D.-H. Lee, Phys. Rev. B **81**, 184512 (2010).
  - [24] R. Thomale *et al.*, Phys. Rev. Lett. **106**, 187003 (2011).
  - [25] K. Suzuki, H. Usui, and K. Kuroki, J. Phys. Soc. Jpn. **80**, 013710 (2011).
  - [26] S. Sharma *et al.*, Phys. Rev. B **81**, 174512 (2010).
  - [27] W. Schnelle *et al.*, Phys. Rev. B **79**, 214516 (2009).
  - [28] F. Rullier-Albenque *et al.*, Phys. Rev. B **81**, 224503 (2010).
  - [29] A. Thaler *et al.*, Phys. Rev. B **82**, 014534 (2010).
  - [30] V. Brouet *et al.*, Phys. Rev. Lett. **105**, 087001 (2010).
  - [31] Man Jin Eom and Jun Sung Kim, to be published.
  - [32] S. Kasahara *et al.*, Phys. Rev. B **81**, 184519 (2010).
  - [33] A. Yamamoto *et al.*, Appl. Phys. Lett. **94**, 062511 (2009).
  - [34] H. Shakeripour *et al.*, New J. Phys. **11**, 055065 (2009).
  - [35] J. Lowell and J. Sousa, J. Low. Temp. Phys. **3**, 65 (1970).
  - [36] C. Proust *et al.*, Phys. Rev. Lett. **89**, 147003 (2002).
  - [37] G. E. Volovik, JETP Lett. **58**, 469 (1993).
  - [38] J.-Ph. Reid *et al.*, Phys. Rev. B **82**, 064501 (2010).
  - [39] W. K. Yeoh *et al.*, Phys. Rev. Lett. **106**, 247002 (2011).
  - [40] M. Tegel *et al.*, arXiv:0805.1208, Z. Naturforsch. B - Chem. Sci. **63**, 1057 (2008).
  - [41] S. Jiang *et al.*, J. Phys. Condens. Matter **21**, 382203 (2009).
  - [42] H. Shishido *et al.*, Phys. Rev. Lett. **104**, 057008 (2010).
  - [43] R. Nath *et al.*, Phys. Rev. B **79**, 174513 (2009).